

Prediction and Use of Contrail Frequency Index for Contrail Reduction Strategies

Neil Y. Chen* and Banavar Sridhar[†]

NASA Ames Research Center, Moffett Field, CA 94035-1000

Hok K. Ng[‡]

University of California, Santa Cruz, Moffett Field, CA 94035-1000

Methods have been proposed to reduce aircraft-induced contrails by on-board sensing and strategic planning. This paper describes a class of indices that predict potential aircraft-induced contrail formations one to six hours in advance. The indices can be used to identify air traffic control centers and altitudes with high potential for contrail formation. The results show that the index is affected more by the changing atmospheric conditions than by small daily variations in the nominal traffic. The analysis shows that the one-hour predicted contrail frequency index is highly correlated with the actual contrail frequency, with an average correlation coefficient of 0.85. The correlation coefficient is lower with longer prediction time, down to 0.52 for six-hour prediction. The average success rates for identifying air traffic control centers and altitudes with high contrail frequency are as high as 83.47% for one-hour prediction.

I. Introduction

CONTRAILS are clouds that are visible trails of water vapor made by the exhaust of aircraft engines. They appear and persist if the aircraft is flying in certain atmospheric conditions. The environmental impact of aircraft-induced persistent contrails has drawn attention in recent years.¹ Persistent contrails reduce incoming solar radiation and outgoing thermal radiation in a way that accumulates heat.² The global mean contrail cover observed in 1992 is estimated to double by 2015 and to quadruple by 2050 due to the increase in air traffic.³ Studies suggest that the environmental impact from persistent contrails may be three to four times,⁴ or even ten times,⁵ larger than that from aviation emissions. Therefore, methods to reduce aircraft-induced persistent contrails need to be explored to minimize the impact on the global environment.

Efforts have been made in the past years to identify and reduce persistent contrail production. Gierens⁶ and Noppel⁷ reviewed various strategies for contrail avoidance including changing engine architecture, enhancing airframe and engine integration, using alternate fuels, and modifying traffic flow management procedures. Among the traffic flow management solutions, Mannstein⁸ proposed a strategy to reduce the climate impact of contrails significantly by small changes to each aircraft's flight altitude. Campbell⁹ presented a mixed integer programming methodology to optimally reroute aircraft trajectories to avoid the formation of persistent contrails. Both methodologies require a flexible flight plan and onboard contrail detection system. Fichter¹⁰ showed that the global annual mean contrail coverage could be reduced by reducing the cruise altitude. Williams^{11,12} proposed strategies for contrail reduction by identifying fixed and varying maximum altitude restrictions. These restrictions generally require more fuel burn and add congestion to the already crowded airspace at lower altitudes.

The objective of this paper is to derive a class of indices that can identify and predict, up to six hours in advance, regions of airspace with high potential for contrail formation. Traffic and weather forecasts were used to generate the predicted contrail frequency index. The indices are used to identify air traffic control centers and altitudes with high contrail formation activities over the next one to six hours. The method

*Research Scientist, U.C. Santa Cruz, MS 210-8, Member

[†]Senior Scientist for Air Transportation Systems, Aviation Systems Division, Fellow.

[‡]Senior Software Engineer, U.C. Santa Cruz, MS 210-8, Member

uses actual air traffic data and provides a one-hour temporal resolution of predicted contrail frequency. The results show that the predicted indices are highly correlated with the actual contrail frequencies and have a high success rate in identifying the centers and flight levels with high contrail frequencies over the next one to three hours.

The remainder of the paper is organized as follows. Section II provides the descriptions of atmospheric and aircraft data and the contrail model used in this paper. Section III describes contrail frequency index, predicted contrail frequency index, and their use for contrail reduction strategies. The results are demonstrated in Section IV. Finally, a summary and conclusions are presented in Section V.

II. Atmospheric and Aircraft Data and Contrail Model

The atmospheric data, contrail model, and aircraft data used to generate the contrail formation frequency are described in this section.

A. Atmospheric Data

Contrails can be observed from surface observation data¹³ and detected by satellite data.¹⁴ Duda¹⁵ has related the observations to numerical weather analysis output and demonstrated that persistent contrail formation can be computed using atmospheric temperature and humidity data retrieved from the Rapid Updated Cycle (RUC) data, provided by the National Oceanic and Atmospheric Administration (NOAA). Contrails can persist when ambient air is supersaturated with respect to ice, which means the environmental relative humidity with respect to ice (RH_i) is greater than one hundred percent.¹⁶ The RH_i can be computed from relative humidity with respect to water (RH_w) and temperature, which are available in the RUC data. The one-hour, two-hour, three-hour, and six-hour forecasts and the forty-kilometer (40km) resolution RUC data were used in this paper. The data have a temporal resolution of one hour, a horizontal resolution of 40 kilometers, and isobaric pressure levels from 100 to 1000 hectopascals (hPa) in 25 hPa increments. The vertical range is from 150 hPa to 400 hPa, which are equivalent to 23,600 feet to 44,400 feet in the standard atmosphere. As an example, snap shots of temperature and RH_w contours at 8AM eastern daylight time (EDT) on August 1, 2007 at a pressure altitude of 250 hPa, or about 34,100 feet, are shown in Fig. 1.

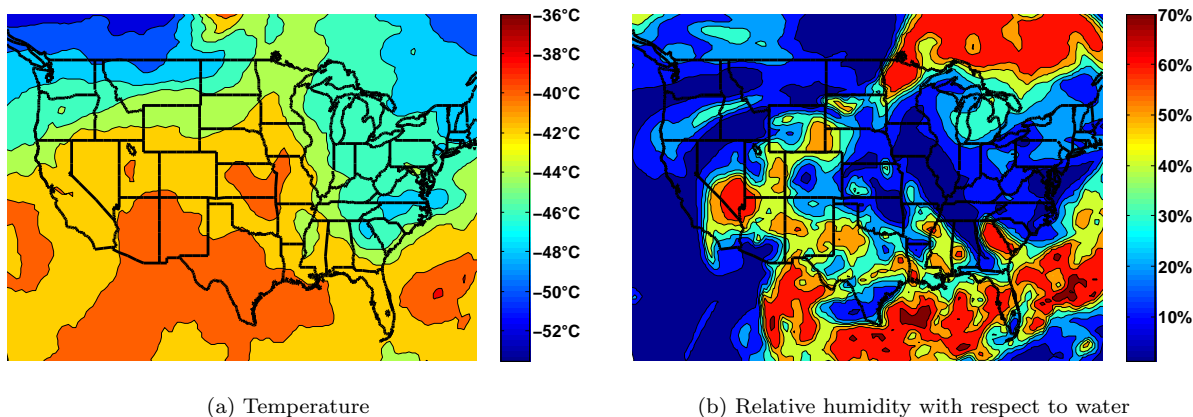


Figure 1. Contours of temperature and RH_w at 34,100 feet at 8AM EDT on August 1, 2007.

B. Contrail Model

Contrails are clouds produced by aircraft operating at high altitudes. Persistent contrail formation areas are defined as areas with RH_i greater than or equal to 100%. RH_i can be computed from RH_w and temperature using the saturation vapor pressure coefficients of Alduchov,¹⁷ formulated as

$$RH_i = RH_w \times \frac{6.0612e^{18.102T/(249.52+T)}}{6.1162e^{22.577T/(237.78+T)}}, \quad (1)$$

where T is the temperature in Celsius. The temperature and relative humidity shown in Fig. 1 can be translated to RH_i.

The 40-km RUC data consist of a grid of (113×151) data points at each isobaric pressure level. The altitude level index, l , is defined as $l = 1 \dots 11$ corresponding to isobaric pressure levels at 400, 375, \dots , 150 hPa. The level index, isobaric pressure level, and approximate corresponding flight levels are listed in Table 1.

Table 1. Altitude level index, isobaric pressure level, and pressure altitude.

level index	1	2	3	4	5	6	7	8	9	10	11
pressure level (hPa)	400	375	350	325	300	275	250	225	200	175	150
flight level (100 feet)	236	251	267	283	301	320	341	363	387	414	444

The potential persistent contrail formation matrix (contrail matrix) at hour h at level l is defined as

$$\mathbf{R}_h^l = \begin{bmatrix} r_{1,1} & r_{1,2} & \dots & r_{1,151} \\ \vdots & \vdots & \ddots & \vdots \\ r_{113,1} & r_{113,2} & \dots & r_{113,151} \end{bmatrix}, \quad (2)$$

where $r_{i,j}$ is 1 if $RHi \geq 100\%$ at grid (i, j) , and 0 if $RHi < 100\%$.

To indicate the location of the twenty U.S. air traffic control centers in the grid, the center grid matrix is defined as

$$\mathbf{C}_k = \begin{bmatrix} c_{1,1} & c_{1,2} & \dots & c_{1,151} \\ \vdots & \vdots & \ddots & \vdots \\ c_{113,1} & c_{113,2} & \dots & c_{113,151} \end{bmatrix}, \quad (3)$$

where k is the center index corresponding to the twenty continental U.S. air space control centers (see Table 2), and $c_{i,j}$ is one if the grid point is within the center and zero if not.

Table 2. Center index of twenty continental U.S. air traffic control centers.

Index	Name	Index	Name
1	Seattle Center (ZSE)	11	Chicago Center (ZAU)
2	Oakland Center (ZOA)	12	Indianapolis Center (ZID)
3	Los Angeles Center (ZLA)	13	Memphis Center (ZME)
4	Salt Lake City Center (ZLC)	14	Cleveland Center (ZOB)
5	Denver Center (ZDV)	15	Washington D. C. Center (ZDC)
6	Albuquerque Center (ZAB)	16	Atlanta Center (ZTL)
7	Minneapolis Center (ZMP)	17	Jacksonville Center (ZJX)
8	Kansas City Center (ZKC)	18	Miami Center (ZMA)
9	Dallas/Fort Worth Center (ZFW)	19	Boston Center (ZBW)
10	Houston Center (ZHU)	20	New York Center (ZNY)

The potential persistent contrail formation coverage ratio (contrail coverage ratio) of one center can be defined by the total area of the contrail regions in the center divided by the area of the center. Assuming all of the grid points have the same area, the contrail coverage ratio of center k at time t at altitude level l can be defined as

$$\frac{\sum_{i=1}^{113} \sum_{j=1}^{151} r_{i,j} c_{i,j}}{\sum_{i=1}^{113} \sum_{j=1}^{151} c_{i,j}}, \quad (4)$$

where $r_{i,j}$ is an element of \mathbf{R}_t^l , and $c_{i,j}$ is an element of \mathbf{C}_k . As an example, the contrail area at flight level 341 at 8AM EDT on August 1, 2007 is shown in Fig. 2a. The corresponding center contrail coverage ratio, computed from Eq. (4), is shown in Fig. 2b. The center contrail coverage ratio indicates the portion of center airspace that would form contrails when aircraft fly through it. When the ratio is zero, there will be no contrail formed in the center.

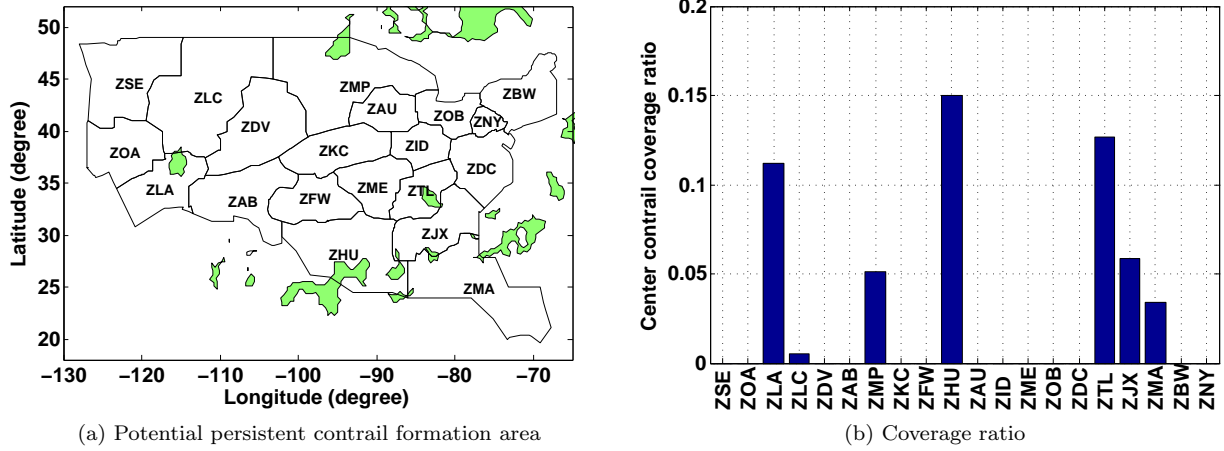


Figure 2. Potential persistent contrail formation area and coverage ratio at flight level 341 at 8AM EDT on August 1, 2007.

C. Aircraft Data

Contrails form when aircraft fly through a potential contrail formation area. Aircraft locations are needed to determine the contrail formation frequency. The aircraft data used in this paper were extracted from the Federal Aviation Administration’s Aircraft Situation Display to Industry (ASDI) data. The ASDI has a sampling rate of one minute. The same grid used in the RUC data was used to generate the aircraft position matrix. The aircraft position matrix is defined as

$$\mathbf{A}_t^l = \begin{bmatrix} a_{1,1} & a_{1,2} & \dots & a_{1,151} \\ \vdots & \vdots & \ddots & \vdots \\ a_{113,1} & a_{113,2} & \dots & a_{113,151} \end{bmatrix}, \quad (5)$$

where $a_{i,j}$ is the number of aircraft within grid (i,j) flying closest to altitude level l at time t . The aircraft position matrix indicates the air traffic density in the grid scale at different altitudes.

III. Methodology

The concept of contrail frequency index, predicted contrail frequency index, and its use for contrail reduction strategies are described in this section.

A. Contrail Frequency Index

As discussed in the previous section, the size and coverage ratio of the persistent contrail formation areas are not sufficient indications of severity of contrail activities. The center contrail frequency index consists of both potential contrail formation area and air traffic information. It is defined as the number of aircraft flying through an area that would form persistent contrails at time t at level l . It is formulated as

$$\sum_{i=1}^{113} \sum_{j=1}^{151} r_{i,j} c_{i,j} a_{i,j}, \quad (6)$$

where $r_{i,j}$, $c_{i,j}$, and $a_{i,j}$ are defined in Eq. (2), (3), and (5).

As an example, the center contrail frequency indices at flight level 341 were computed at 8AM EDT on August 1, 2007 and are shown in Fig. 3. Even though in Fig. 2b the contrail coverage ratio of Houston Center is higher than Atlanta Center, in Fig. 3 the contrail frequency of Houston Center is zero. Figure 4a and 4b show the aircraft locations and contrail areas of Houston and Atlanta Center. The green dots indicate the aircraft trajectories of 8AM EDT. The contrail areas are shown in blue contours. The red dots show the aircraft inside the contours. Houston Center has larger contrail areas, but no aircraft flying through the

contours, while there are more aircraft flying through the contours at Atlanta Center. The center contrail frequency is 0 in Houston Center and 109 in Atlanta Center. This example shows that the center contrail coverage ratio does not reflect the actual severity of contrail frequency in a center. With aircraft location, the contrail frequency can indicate the severity of the persistent contrail formation.

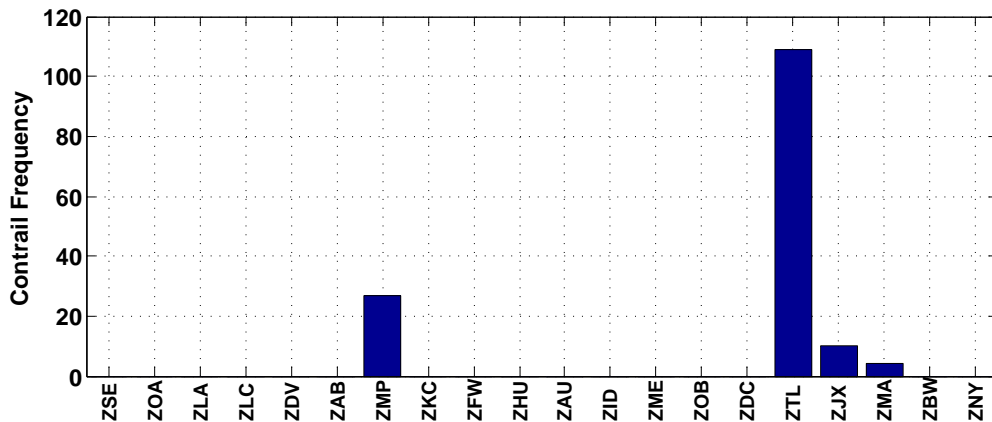
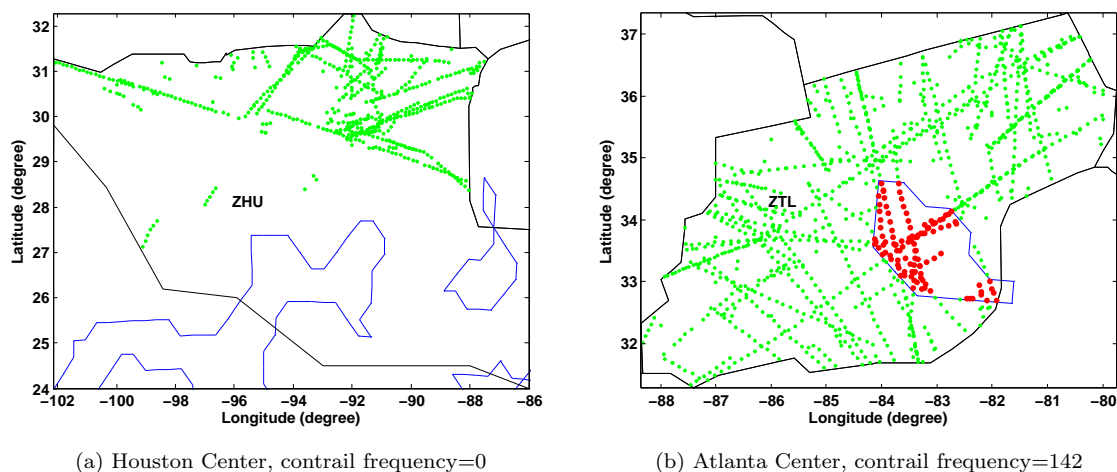


Figure 3. Center contrail frequencies at flight level 341 at 8AM EDT on August 1, 2007.



(a) Houston Center, contrail frequency=0 (b) Atlanta Center, contrail frequency=142
Figure 4. Aircraft location and persistent contrail formation areas at 8AM EDT on August 1, 2007.

B. Predicted Contrail Frequency Index

The contrail frequency index derived in the previous section indicates the actual contrail activities. For strategic planning, prediction of the contrail frequency for the next few hours is needed. The predicted contrail frequency index is defined as a convolution of traffic data and atmospheric conditions. They are similar to the concept of Weather Impacted Traffic Index (WITI) introduced by Callaham et al.¹⁸ and Sridhar,¹⁹ and the three dimensional index derived by Chen.²⁰ The index consists of the RUC forecast data and the predicted aircraft locations. The center predicted contrail frequency index is defined as the predicted number of aircraft flying through the forecasted potential contrail area at time t at level l in center k . It is formulated as

$$\sum_{i=1}^{113} \sum_{j=1}^{151} r'_{i,j} c_{i,j} a'_{i,j}, \quad (7)$$

where $r'_{i,j}$ is defined in Eq. (2) with RUC forecast data, $c_{i,j}$ is defined in (3), and $a'_{i,j}$ is defined in (5). $a'_{i,j}$ is based on the historic air traffic data during the planning period. As in the case of WITI, the index is

affected more by the changing atmospheric conditions than by small daily variations to the nominal traffic plan.¹⁹ In Eq. (7) the coefficient $a'_{i,j}$ can be thought of as an air traffic weighting coefficient.

C. Contrail Reduction Strategy

The feasibility of using predicted contrail frequency index for contrail reduction is investigated. The center predicted contrail frequency index can be used to identify the flight level that would have formed the most contrails and find an alternate altitude with less contrail activities. The contrail frequency index after the contrail reduction strategy has been applied is formulated as

$$\sum_{i=1}^{113} \sum_{j=1}^{151} r_{i,j} c_{i,j} \hat{a}_{i,j}, \quad (8)$$

where $r_{i,j}$ and $c_{i,j}$ are defined in Eqs. (2) and (3), and $\hat{a}_{i,j}$ is defined in Eq. (5) with the aircraft location after the contrail reduction strategy is applied.

The contrail reduction strategies need to consider extra fuel burn to minimize overall environmental impact and not to add congestions in the center. The strategy in Ref. 21 uses the predicted contrail frequency index to identify the area that would have formed the most contrail activities, and change the cruise altitudes of a group of aircraft to reduce contrails. The changes need to have minimal extra fuel utilization and maintain the air traffic density below airspace capacity. In general, changing the cruise altitude of a group of aircraft will not increase the air traffic density within the center and sectors.

IV. Results

The temperature and relative humidity from RUC data and aircraft position from ASDI data in 2007 were processed and analyzed. Figure 5 shows four average hourly indices at each of the twenty continental U.S. centers at different altitudes in 2007. They are the contrail coverage ratio derived in Section II.B, the aircraft position matrix derived in Section II.C, the contrail frequency index derived in Section III.A, and the contrail frequency density derived later in this section. As shown in the figure, most of the contrails were formed between flight level 301 and 387. These flight levels account for 78% of contrail frequency over all centers and altitudes. Seattle Center (ZSE), Oakland Center (ZOA), Los Angeles Center (ZLA), and New York Center (ZNY) have lower contrail activities. The reasons are there are less flight activities at ZSE, ZOA, and ZLA, and the size of ZNY is small bringing the index low. To observe the density of the center contrail frequency index, the center contrail frequency density is defined by the center contrail frequency index divided by the number of grid points in the center, formulated as

$$\frac{\sum_{i=1}^{113} \sum_{j=1}^{151} r_{i,j} c_{i,j} a_{i,j}}{\sum_{i=1}^{113} \sum_{j=1}^{151} c_{i,j}}, \quad (9)$$

where $r_{i,j}$, $c_{i,j}$, and $a_{i,j}$ are defined in Eq. (2), (3), and (5). Figure 5d shows the average hourly center contrail frequency density at each of the eleven flight levels and twenty centers. It is shown that there are high contrail activities between flight level 320 and 363, having some centers with density higher than 0.5. The highest contrail density is 0.69 at flight level 363 at Indianapolis Center (ZID). Figure 6 shows the contrail frequency density at flight level 363 on a U.S. map. As shown in the figures, Indianapolis Center (ZID) has the highest contrail density, and its surrounding five centers, Kansas City Center (ZKC), Chicago Center (ZAU), Memphis Center (ZME), Cleveland Center (ZOB), and Atlanta Center (ZTL), also have high contrail density ranged from 0.45 to 0.57. The seasonal variation can be observed by the monthly average center contrail frequency at ZID in 2007, as shown in Fig. 7. In general, there are less contrail activities in summer. The contrail frequency index provides a way to quantify the contrail activities.

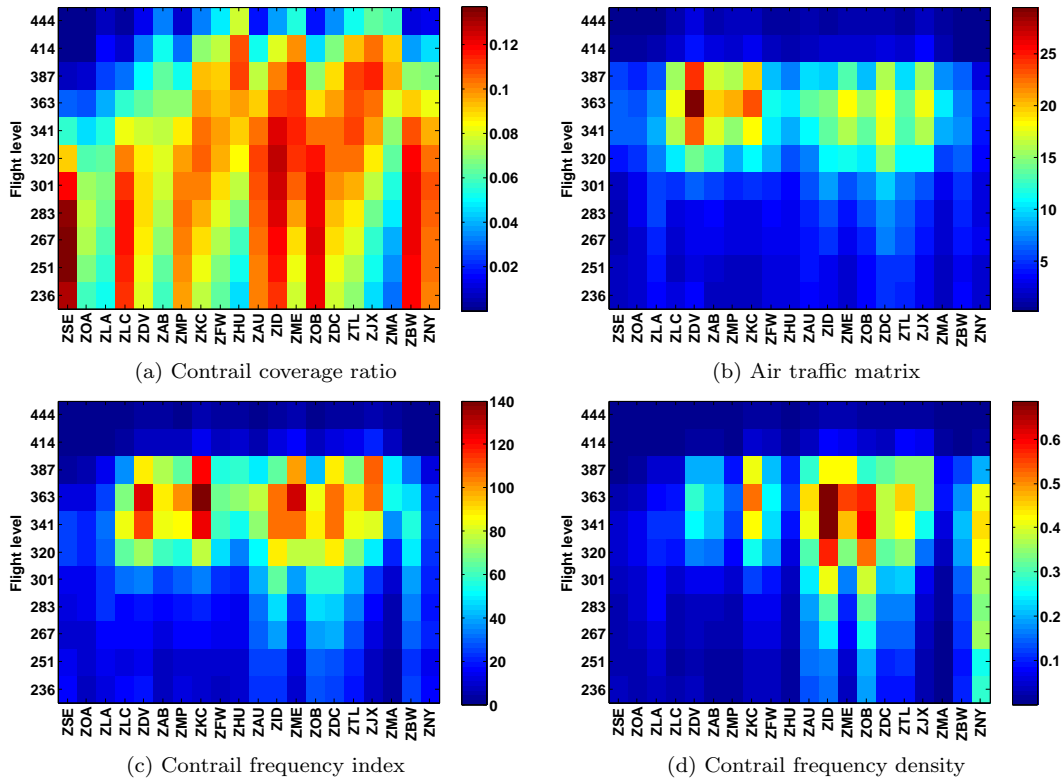


Figure 5. Average hourly center contrail coverage ratio, air traffic density, contrail frequency and contrail frequency density in 2007.

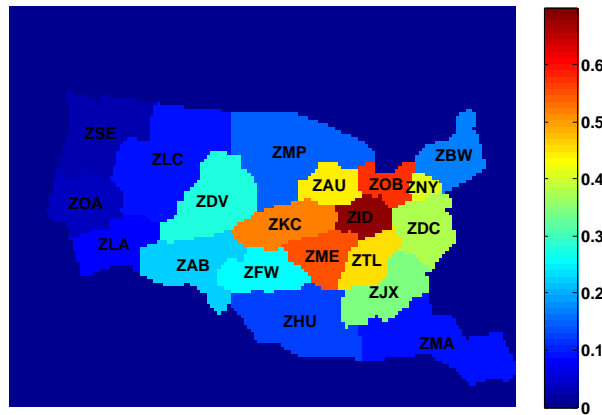


Figure 6. Center contrail frequency density at flight level 363 in 2007.

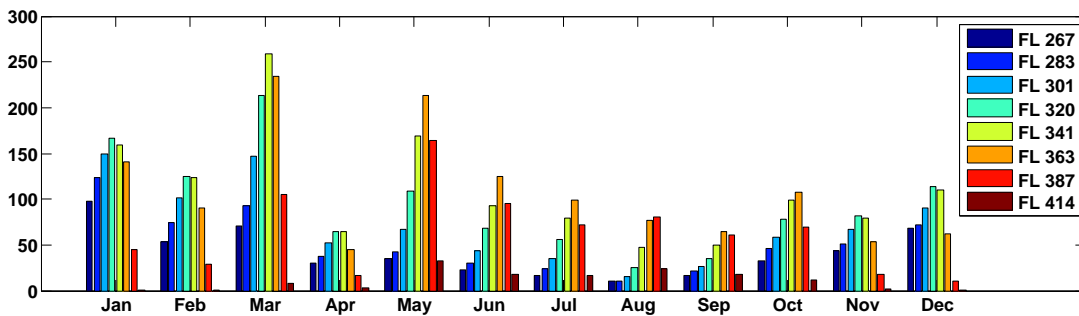
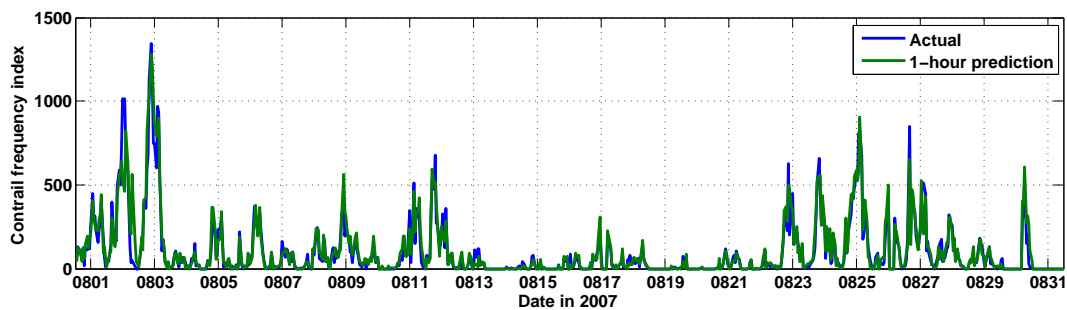


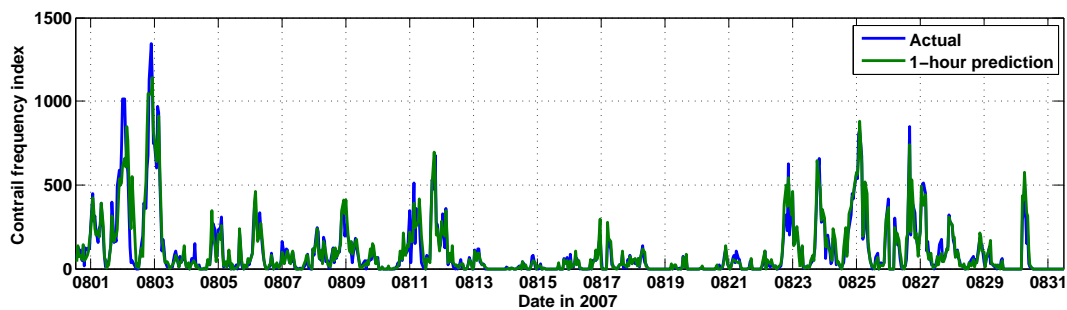
Figure 7. Monthly average hourly contrail frequency at Indianapolis Center in 2007.

Next, for the predicted contrail frequency index, one-hour, two-hour, three-hour, and six-hour predicted indices in August 2007 were generated using Eq. (7) and analyzed. $a'_{i,j}$ in Eq. (7) was based on the air traffic data on the same day of week of July 15-21. For example, to generate the predicted contrail frequency indices on August 1, 8, 15, 22, and 29, the air traffic data on July 18 was used since they are all Wednesdays. As an example, actual and one-hour predicted contrail frequency indices at flight level 363 at Indianapolis center are shown in Fig. 8a. As shown in the figure, the one-hour predicted contrail index is highly correlated with actual index, with a correlation coefficient of 0.94. It is mentioned in Ref. 19 that the index is affected more by the changing atmospheric conditions than by small daily variations to the nominal traffic plan.

To show the effect on different choices of the historical air traffic data used, the predicted contrail frequency index was regenerated using $a'_{i,j}$ computed by the average air traffic in July 2007. The indices at flight level 363 at Indianapolis Center using the average traffic in July 2007 are shown in Fig. 8b with a correlation coefficient of 0.94. The result is very similar to using the air traffic data on July 15-21. Table 3 shows the average correlation coefficients between actual and predicted indices in twenty centers at different flight levels using historical data of July 15-21 and the average of July 2007. Note that there is no significant difference between the two types of historical data. The accuracy of the prediction decays with longer prediction time. The correlations at flight level 414 and 444 are small mainly because of the lower frequency of contrail formation and the resulting higher sensitivity to the noise. The mean correlation coefficients between actual index and one-hour, two-hour, three-hour, and six-hour predicted index are 0.85, 0.72, 0.64, and 0.52 using July 15-21 data, and 0.84, 0.72, 0.63, and 0.51 respectively.



(a) Use of air traffic data on July 15-21, 2007



(b) Use of average air traffic data in July 2007

Figure 8. Actual and predicted center contrail frequency index at flight level 363 at Indianapolis Center in August 2007.

To use the prediction contrail frequency index for contrail reduction strategies, center prediction indices were generated and analyzed. Figure 9 shows the actual and predicted center contrail frequency indices at flight level 363 at 8PM EDT on August 1, 2007. The blue bars are the actual, and the light blue, green, orange, and red color bar are the one-hour, two-hour, three-hour, and six-hour predicted contrail frequency indices computed by Eq. (7) using traffic data on July 18, 2007. As shown in the figure, the actual contrail frequency index and the one-hour, two-hour, and three-hour predicted contrail frequency indices are correlated. In general, when the actual contrail frequency is high, the predicted contrail frequency is high for prediction up to three hours. The six-hour predicted index is under-predicted, most likely due to the prediction inaccuracy.

For implementing a contrail reduction strategy, the centers with high contrail frequency indices need to be identified. As an example, the contrail reduction strategy may be enabled when the centers have indices

Table 3. Average correlation coefficient between actual and predicted contrail frequency index over twenty U.S. centers in August 2007. Two types of historical data are used, air traffic on July 15-21, 2007 (ref. 1) and the average air traffic in July 2007 (ref. 2).

flight level	prediction time							
	one-hour		two-hour		three-hour		six-hour	
	ref. 1	ref. 2	ref. 1	ref. 2	ref. 1	ref. 2	ref. 1	ref. 2
444	0.64	0.63	0.58	0.57	0.53	0.53	0.46	0.46
414	0.73	0.69	0.66	0.63	0.60	0.57	0.54	0.50
387	0.89	0.90	0.81	0.82	0.73	0.74	0.57	0.58
363	0.92	0.92	0.79	0.79	0.70	0.69	0.55	0.54
341	0.91	0.91	0.77	0.77	0.68	0.68	0.53	0.52
320	0.91	0.90	0.77	0.75	0.68	0.67	0.53	0.53
301	0.88	0.88	0.73	0.74	0.65	0.65	0.53	0.53
283	0.86	0.86	0.71	0.71	0.62	0.61	0.50	0.48
267	0.86	0.84	0.70	0.70	0.62	0.61	0.49	0.48
251	0.86	0.85	0.70	0.70	0.63	0.62	0.50	0.50
236	0.87	0.86	0.71	0.71	0.63	0.61	0.50	0.48

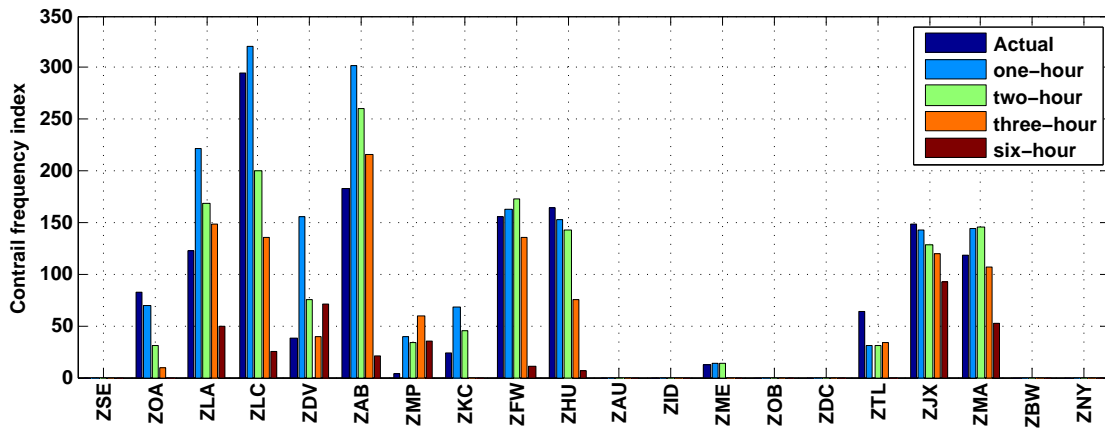


Figure 9. Actual and predicted center contrail frequency index at flight level 363 at 8PM EDT on August 1, 2007.

higher than 100. This would affect seven centers including Los Angeles Center (ZLA), Salt Lake City Center (ZLC), Albuquerque Center (ZAB), Dallas/Fort Worth Center (ZFW), Houston Center (ZHU), Jacksonville Center (ZJX), and Miami Center (ZMA). All of the one-hour, two-hour, and three-hour prediction indices are able to correctly identify the centers that need a reduction strategy with the exception that the three-hour predicted index fails to identify ZHU. There is one case that the one-hour prediction falsely identifying Denver Center (ZDV) with low contrail activity as having an index greater than 100. The success rate of the identification is defined as the rate of the predicted contrail index correctly identifying the center with high or low contrail activities. In this example, the one-hour, two-hour, three-hour, and six-hour predicted indices have success rates of 95%, 100%, 95% and 65% for identifying the correct centers respectively.

The performance of predicted indices for identifying centers with high contrail frequency index is shown in Table 4. As expected, the success rate decays with longer prediction time due to the prediction inaccuracy. Also noticeable is that the success rate decays with higher threshold. There is a 83.47% success rate to identify centers with contrail frequency index greater than 100 using one-hour predicted index, 69.24% using two-hour index, 58.31% using three-hour index, and down to 38.92% using six-hour index. It is harder to successfully identify centers with index greater than 400. There is a 76.19% success rate using one-hour index, and down to 21.99% using six-hour index.

Table 4. Success percentage of identifying the center with index greater than the threshold index for twenty U.S. centers in August 2007.

threshold	prediction time			
	one-hour	two-hour	three-hour	six-hour
100	83.47%	69.24%	58.31%	38.92%
200	81.43%	64.37%	51.27%	30.69%
300	79.14%	60.75%	46.36%	26.18%
400	76.19%	57.28%	41.69%	21.99%

V. Conclusions

This paper described a methodology to predict contrail frequency index for contrail reduction. A class of predicted indices that reflects the severity of airspace contrail formation frequency was derived. The indices consist of weather forecast and actual and historical air traffic data. The results show that the predicted indices are affected more by changing atmospheric conditions than by small daily variations of traffic. For the data tested, the one-hour predicted contrail index is highly correlated with the actual index, resulting in an average correlation coefficient of 0.85 and is lower with longer prediction time. The average correlation coefficient between the actual index and the two-hour, three-hour, and six-hour predicted index are 0.72, 0.64, and 0.52, respectively. In terms of developing strategies for contrail reduction, there is a 83.47% success rate to identify centers with contrail frequency index greater than a threshold, 69.24% using two-hour index, 58.31% using three-hour index, and 38.92% using six-hour index. The method of using predicted contrail frequency index for contrail reduction shows promise but requires detailed future evaluation in a fast-time traffic flow management simulation environment.

References

- ¹Waitz, I., Townsend, J., Cutcher-Gershenfeld, J., Greitzer, E., and Kerrebrock, J., "Report to the United States Congress: Aviation and the Environment, A National Vision, Framework for Goals and Recommended Actions," Tech. rep., Partnership for AiR Transportation Noise and Emissions Reduction, London, UK, December 2004.
- ²Meerkotter, R., Schumann, U., Doelling, D. R., Minnis, P., Nakajima, T., and Tsushima, Y., "Radiative forcing by contrails," *Annales Geophysicae*, Vol. 17, 1999, pp. 1080–1094.
- ³Marquart, S., Ponater, M., Mager, F., and Sausen, R., "Future Development of Contrail Cover, Optical Depth, and Radiative Forcing: Impacts of Increasing Air Traffic and Climate Change," *Journal of Climate*, Vol. 16, September 2003, pp. 2890–2904.
- ⁴"The Environmental Effects of Civil Aircraft in Flight," Tech. rep., Royal Commission on Environmental Pollution, London, UK, 2002.
- ⁵Mannstein, H. and Schumann, U., "Aircraft induced contrail cirrus over Europe," *Meteorologische Zeitschrift*, Vol. 14, No. 4, 2005, pp. 549–554.
- ⁶Gierens, K., Limb, L., and Eleftheratos, K., "A Review of Various Strategies for Contrail Avoidance," *The Open Atmospheric Science Journal*, Vol. 2, 2008, pp. 1–7.
- ⁷Noppel, F. and Singh, R., "Overview on Contrail and Cirrus Cloud Avoidance Technology," *Journal of Aircraft*, Vol. 44, No. 5, 2007, pp. 1721–1726.
- ⁸Mannstein, H., Spichtinger, P., and Gierens, K., "A note on how to avoid contrail cirrus," *Transportation Research. Part D, Transport and environment*, Vol. 10, No. 5, September 2005, pp. 421–426.
- ⁹Campbell, S. E., Neogi, N. A., and Bragg, M. B., "An Optimal Strategy for Persistent Contrail Avoidance," *AIAA Guidance, Navigation and Control Conference*, AIAA-2008-6515, AIAA, Honolulu, HI, August 2008.
- ¹⁰Fichter, C., Marquart, S., Sausen, R., and Lee, D. S., "The impact of cruise altitude on contrails and related radiative forcing," *Meteorologische Zeitschrift*, Vol. 14, No. 4, August 2005, pp. 563–572.
- ¹¹Williams, V., Noland, R. B., and Toumi, R., "Reducing the climate change impacts of aviation by restricting cruise altitudes," *Transportation Research. Part D, Transport and environment*, Vol. 7, No. 5, November 2002, pp. 451–464.
- ¹²Williams, V. and Noland, R. B., "Variability of contrail formation conditions and the implications for policies to reduce the climate impacts of aviation," *Transportation Research. Part D, Transport and environment*, Vol. 10, No. 4, July 2005, pp. 269–280.
- ¹³Minnis, P., Ayers, J. K., Nordeen, M. L., and Weaver, S. P., "Contrail Frequency over the United States from Surface Observations," *Journal of Climate*, Vol. 16, No. 21, November 2003, pp. 34473462.
- ¹⁴Palikonda, R., Minnis, P., Duda, D. P., and Mannstein, H., "Contrail coverage derived from 2001 AVHRR data over the continental United States of America and surrounding areas," *Meteorologische Zeitschrift*, Vol. 14, No. 4, August 2005, pp. 525–536.

¹⁵Palikonda, R., Minnis, P., Duda, D. P., and Mannstein, H., “Relating observations of contrail persistence to numerical weather analysis output,” *Atmospheric Chemistry and Physics*, Vol. 9, No. 4, February 2009, pp. 1357–1364.

¹⁶Duda, D. P., Minnis, P., Costulis, P. K., and Palikonda, R., “CONUS Contrail Frequency Estimated from RUC and Flight Track Data,” *European Conference on Aviation, Atmosphere, and Climate*, Friedrichshafen at Lake Constance, Germany, June-July 2003.

¹⁷Alduchov, O. A. and Eskridge, R. E., “Improved Magnus Form Approximation of Saturation Vapor Pressure,” *Journal of Applied Meteorology*, Vol. 35, No. 4, April 1996, pp. 601–609.

¹⁸Callahan, M. B., DeArmon, J. S., Cooper, A., Goodfriend, J. H., Moch-Mooney, D., and Solomos, G., “Assessing NAS Performance: Normalizing for the Effects of Weather,” *4th USA/Europe Air Traffic Management R&D Symposium*, Santa Fe, NM, December 2001.

¹⁹Sridhar, B. and Swei, S., “Relationship between Weather, Traffic and Delay Based on Empirical Methods,” *6th AIAA Aviation Technology, Integration and Operations Conference (ATIO)*, Wichita, KS, September 2006.

²⁰Chen, N. Y. and Sridhar, B., “Estimation of Air Traffic Delay Using Three Dimensional Weather Information,” *8th AIAA Aviation Technology, Integration and Operations Conference (ATIO)*, Anchorage, AK, September 2008.

²¹Sridhar, B., Chen, N. Y., and Ng, H. K., “Fuel Efficient Strategies for Reducing Contrail Formations in United State National Air Space,” *29th Digital Avionics Systems Conference*, Salt Lake City, UT, October 2010, to appear.